

# Theoretical study on the structures, isomerization and stability of SiC<sub>3</sub>H isomers

Hao Sun · Nannan Tan · Hongqing He · Xiumei Pan ·  
Zhongmin Su · Rongshun Wang

Received: 1 February 2008 / Accepted: 2 February 2008 / Published online: 29 February 2008  
© Springer-Verlag 2008

**Abstract** The calculations of the geometry optimizations, energies, dipole moments, vibrational spectra, rotational constants, and isomerization of doublet SiC<sub>3</sub>H species were performed using density functional theory and ab initio methods. Four types of isomers, a total of 18 minima, connected by 16 interconversion transition states, were located on the potential energy surface (PES) at the B3LYP/6-311G (d, p) level. More accurate energies were obtained at the CCSD(T)/6-311G(2df, 2p), and G3(MP2) levels. With the highest isomerization barrier, the lowest lying structure, linear A1 possesses the largest kinetic stability. Besides, the isomerization barriers of A2, A4, C2, F1, F4 and F5 are over 10 kcal/mol, and these isomers are also considered to be higher kinetically stable. Other isomers cannot be kinetically stabilized with considerably low isomerization barriers. Investigation on the bonding properties and the computations of vibrational spectra, dipole moments, and rotational constants for SiC<sub>3</sub>H isomers are helpful for understanding their structures and also valuable for their detections in the interstellar space and laboratory.

**Keywords** SiC<sub>3</sub>H · Potential energy surface · Isomer · Stability

H. Sun · N. Tan · X. Pan · Z. Su · R. Wang (✉)  
Institute of Functional Material Chemistry,  
Faculty of Chemistry, Northeast Normal University,  
Renmin Road 5268, Changchun,  
Jilin 130024, People's Republic of China  
e-mail: wangrs@nenu.edu.cn

H. He  
State Key Laboratory of Magnetic Resonance  
and Atomic and Molecular Physics, Wuhan Institute of Physics  
and Mathematics, Chinese Academy of Sciences, Wuhan 430071,  
People's Republic of China

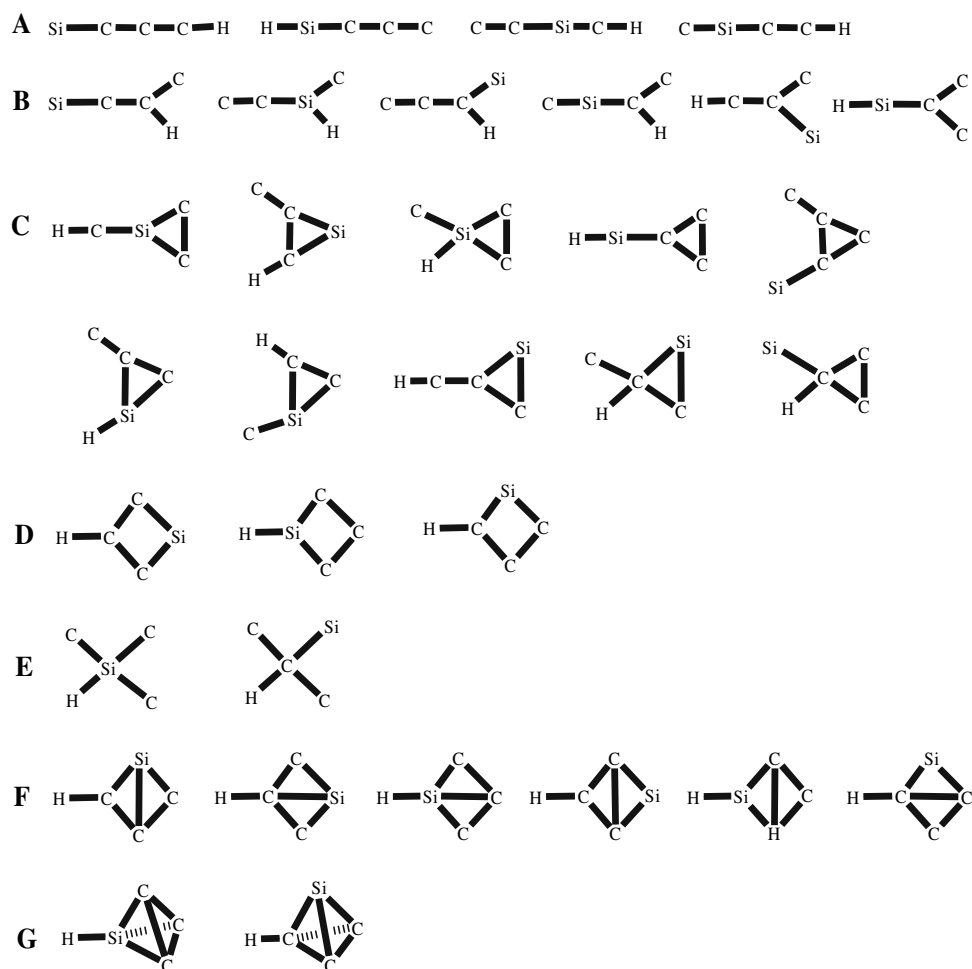
## 1 Introduction

Due to the excellent characters, such as high intensity, endurance to high temperature and oxygenation and regulable resistance, silicon–carbon species play an important role in the field of the material chemistry [1–6], and consequently, small silicon–carbon clusters have attracted extensive attention of the worldwide chemists recent years [7–11]. SiC<sub>n</sub>X (X = N, P, H etc.) species are also speculated as the connection between SiC<sub>n</sub> and C<sub>n</sub>X. As we know, both silicon and carbon atom may be either singly or multiply bonded to the adjacent atoms in the cluster, which results in a large number of chain and ring isomers of considerable stability. The investigation on the isomers and their conversions of the interstellar silicon–carbon clusters (SiC<sub>n</sub>X) is greatly beneficial for exploring the new silicon–carbon species in laboratory or interstellar space, and the mechanism of silicon–carbon material formation as well. Furthermore, many small silicon–carbon clusters, SiC<sub>n</sub>H ( $n = 1–3$ ) and SiCN, for example, have been proved to exist in the interstellar space [12–15]. Because of their close relationship with the star evolution, research on the interstellar molecules, SiC<sub>n</sub>X, is helpful to investigate the nebulae characteristics and reveal the arcanum of life-origin [16–20].

Based on the theoretical results, such as rotational constant and geometry, SiC<sub>n</sub>H, SiCN and SiNC were detected in the laboratory by McCarthy et al. [7]. In their report, McCarthy also suggested that SiC<sub>3</sub>H should be detectable in the laboratory. Up to our knowledge, there is no evidence of a follow-up study in print.

In the present work, we focused our interest on the SiC<sub>3</sub>H cluster. Quantum chemistry method was used to study structures, spectroscopies, isomerization and stability of SiC<sub>3</sub>H, and bonding properties as well. Therefore, our computational work may provide theoretical foundation for future

**Fig. 1** All the initially designed structures for  $\text{SiC}_3\text{H}$  isomers optimizations



experimental detection of  $\text{SiC}_3\text{H}$ , and enrich the information and property of  $\text{SiC}_n\text{H}$  system.

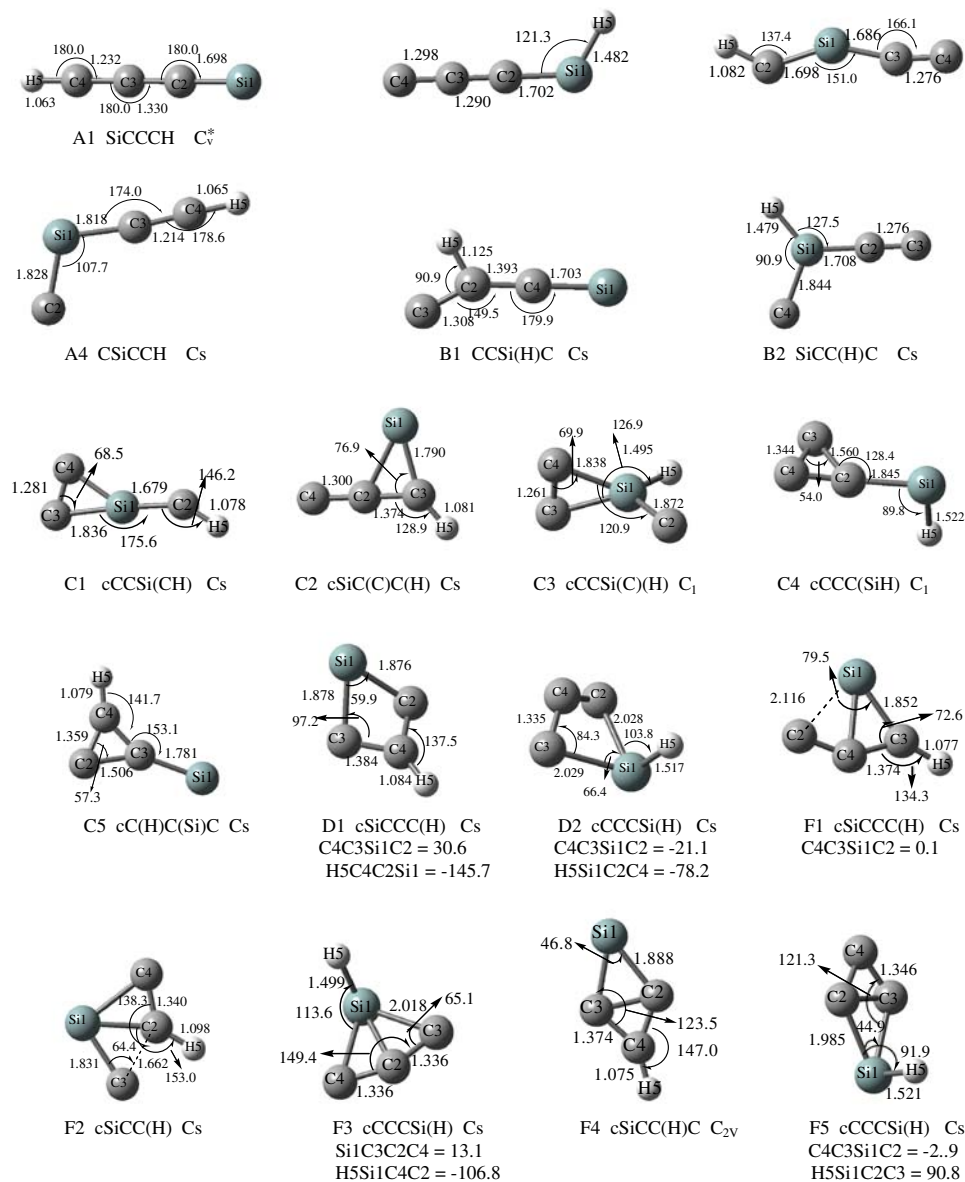
## 2 Computational methods

All of the electronic structure calculations were carried out using the Gaussian 03 program [21]. It is well known that DFT method with considerable basis set can predict accurate geometries for many systems, including interstellar molecule and radicals. DFT/B3LYP method [22–24] was successfully used to investigate the isomerization of similar systems,  $\text{SiC}_3\text{P}$ ,  $\text{SiC}_3\text{N}$  and  $\text{PC}_3\text{P}$  [25–27]. Therefore, the isomerization of  $\text{SiC}_3\text{H}$  was explored using DFT/B3LYP method with the 6-311G(d, p) basis set [28,29] in the present work. The optimized geometries, harmonic vibrational frequencies and zero-point energy (ZPE) of 18 local minima and 16 transition states were calculated at the DFT/B3LYP/6-311G(d, p) level of theory. The connections between isomers were

confirmed by the intrinsic reaction coordinate (IRC) calculations [30–32] at the same level. To acquire the more reliable energies, the CCSD(T)/6-311G(2df, 2p) single point energy calculations were performed using the B3LYP/6-311G(d, p) geometries. The energies discussed in the present work are at the CCSD(T)/6-311G(2df, 2p)//B3LYP/6-311G(d, p) + ZPE level, and the values in the parentheses are obtained at the G3(MP2)//B3LYP/6-311G(d, p) + ZPE level, unless otherwise stated.

The major problem in the application of unrestricted spin formalism is that of contamination with higher spin states. The severe spin contamination could lead to a deteriorated estimation of the barrier height [33,34]. We examined the spin contamination before and after annihilation for all species involved in the title reactions. The values of  $\langle S^2 \rangle$  for doublet range from 0.75 to 0.799 before annihilation, while after annihilation  $\langle S^2 \rangle$  is 0.75 (the exact value for a pure doublet). Consequently, the wave function is not severely contaminated by states of higher multiplicity.

**Fig. 2** Optimized geometries of SiC<sub>3</sub>H isomers at the DFT/B3LYP/6-311G(d, p) level (bond length unit: angstrom, bond angle unit: degree)



### 3 Results and discussion

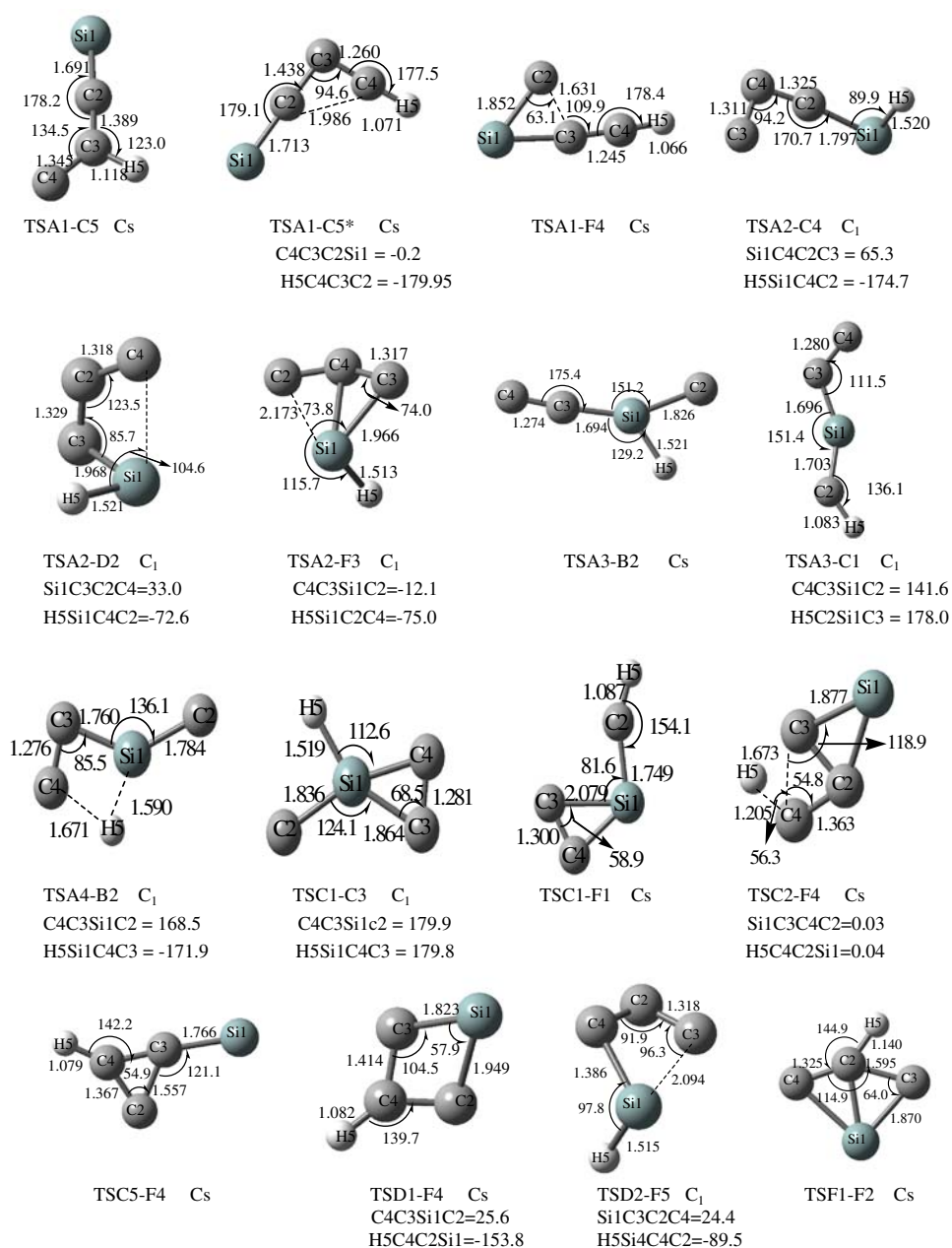
As shown in Fig. 1, seven possible types of isomers, total 33, i.e. chain-like species (A), branched species (B), three-membered-ring species (C), four-membered-ring species (D), tetrahedron species (E), bridge-bond containing species (F) and triangular cone (G) were initially designed. However, only 18 isomers and 16 transition states were theoretically located. TSX-Y denotes the transition states connecting the species X and Y. The optimized geometries of all the local minima and transition states are depicted in Figs. 2 and 3, respectively. Table 1 lists the harmonic vibrational frequencies, the infrared intensities, dipole moments, and rotational constants of all the minima, and the harmonic vibrational

frequencies of transition states are listed in Table 2. The relative energies of all isomers and transition states are summarized in Tables 3 and 4. The potential energy surface (PES) of the isomerization of SiC<sub>3</sub>H species is depicted in Fig. 4.

#### 3.1 SiC<sub>3</sub>H isomers

For chain-like isomers, all the four chain-like isomers (A1, A2, A3 and A4) and two of six initially designed structures with a branch (B1 and B2), were located. With Si and H standing at the two terminals, linear A1 is the most stable isomers. Therefore, A1 (0.0) is considered the most promising molecule to be detected in the atmosphere or laboratory.

**Fig. 3** Optimized geometries of  $\text{SiC}_3\text{H}$  transition states at the B3LYP/6-311G(d, p) level (bond length unit: angstrom, bond angle unit: degree)



The relative energies of A2, A3 and A4 are 43.91(45.86), 84.09(86.87) and 74.01(78.19) kcal/mol, respectively. All these chain-like isomers are planar structure with  $C_s$  symmetry except that A1 has  $C_{\infty v}$  symmetry with a  $^2\Pi$  electronic state. A2 has a  $^2A'$  electronic state, and A3 and A4 correspond to the  $^2A''$  electronic state. The two isomers with a branch are marked as B1 (57.1 (57.07)) and B2 (109.93 (106.61)), with H atoms bonded with C(2) of C–C–Si frame and Si of C–Si–C–C frame, respectively. Both B1 and B2 are  $C_s$  symmetrized with the  $^2A''$  electronic state.

Although much effort had been taken to search all the ten supposed three-membered-ring structures, only five isomers

were located as minima. Isomers C1 (85.15 (88.46)), C2 (16.94 (17.26)) and C3 (86.31 (88.28)) have a CCSi ring, while, C4 (58.36 (53.23)) and C5 (23.85 (25.48)) have a CCC ring. C1, C2 and C5 are in  $C_s$  symmetry with the  $^2A''$  electronic state. Isomers, C2 and C5, whose branches are dispersedly bonded with three-membered-ring, have lower energies, whereas the energies of C1 and C3, whose branches are bonded only with Si atom, are much higher.

Two four-membered-ring isomers, D1 (25.73 (26.15)) and D2 (65.89 (67.00)), whose H atoms are, respectively, bonded with C opposite to Si and Si atom, were located.

**Table 1** Harmonic vibrational frequencies ( $\text{cm}^{-1}$ ), infrared intensities ( $\text{km/mol}$ ) (in parentheses), dipole moment (D) and rotational constants (GHz) of  $\text{SiC}_3\text{H}$  isomers at the B3LYP/6-311G(d, p) level

Isomers	Frequencies (infrared intensity)	Dipole moment	Rotational constant
A1	156(4), 173(10), 377(64), 453(1), 514(1), 641(17), 642(27), 1457(21), 1988(4)	0.7731	2.608561
A2	143(4), 183(0), 345(9), 487(10), 628(28), 647(5), 1376(3), 1973(446), 2206(10)	5.1695	328.06786, 2.69685, 2.67486
A3	80(0), 98(4), 219(10), 364(17), 542(77), 710(710), 1047(12), 1934(576), 3245(11)	4.9852	194.87076, 3.21552, 3.16333
A4	101(18), 205(6), 279(19), 605(61), 656(45), 757(14), 781(8), 2080(46), 3455(59)	2.7981	25.23674, 3.78579, 3.29196
B1	118(16), 239(21), 265(19), 617(3), 626(6), 830(0), 1361(20), 1733(42), 2825(46)	2.4923	136.75815, 2.71362, 2.66082
B2	66(13), 119(0), 189(16), 427(23), 684(28), 743(13), 786(7), 1924(434), 2244(46)	5.0392	22.54659, 4.11119, 3.47716
C1	137(34), 176(25), 346(5), 374(19), 473(122), 706(54), 1121(55), 1726(4), 3288(23)	2.5490	47.73822, 4.85300, 4.40517
C2	62(2), 352(1), 496(73), 649(49), 780(20), 1019(7), 1076(20), 1768(98), 3200(3)	3.8867	16.19493, 6.42179, 4.59839
C3	74(4), 160(31), 299(67), 510(32), 658(38), 751(17), 832(107), 1831(5), 2214(72)	2.7499	20.97647, 5.39069, 5.11727
C4	90(2), 281(0), 316(0), 541(2), 560(47), 786(72), 1257(3), 1678(13), 2061(156)	2.3623	35.68932, 4.00146, 3.71858
C5	128(2), 317(0), 559(10), 814(17), 819(0), 966(6), 1143(9), 1577(3), 3245(2)	2.8813	36.88192, 4.01880, 3.62392
D1	325(7), 441(31), 540(24), 789(62), 883(9), 922(34), 1142(2), 1442(24), 2068(5)	1.0212	20.73818, 7.16327, 5.72376
D2	184(39), 287(41), 437(6), 502(18), 572(8), 730(9), 1340(129), 1355(3), 2064(216)	0.9614	15.20625, 7.78642, 5.56415
F1	257(10), 401(1), 441(35), 631(9), 709(55), 950(50), 1159(6), 1622(6), 3262(4)	3.5508	12.21451, 10.43418, 5.62723
F2	240(77), 290(18), 382(8), 579(45), 600(47), 714(4), 780(5), 1352(12), 3059(86)	1.3579	13.01137, 9.97103, 5.64505
F3	201(41), 347(8), 457(0), 510(18), 668(17), 789(33), 1164(0), 1461(23), 2095(44)	2.4007	12.17557, 10.27842, 5.78271
F4	334(45), 366(8), 564(19), 612(15), 908(6), 965(20), 1027(1), 1563(40), 3289(37)	1.5837	37.43901, 5.69538, 4.94337
F5	274(24), 339(2), 500(16), 632(10), 743(18), 872(26), 1192(1), 1632(70), 2050(204)	0.2265	31.49658, 5.58778, 4.95445

**Table 2** Harmonic vibrational frequencies ( $\text{cm}^{-1}$ ) of all the transition states on the isomerization PES at the B3LYP/6-311G(d, p) level

TSSs	Frequencies (infrared intensity)
TSA1-C5	346i, 213, 217, 583, 654, 958, 1416, 1603, 2843
TSA1-C5*	631i, 241, 254, 547, 669, 858, 1316, 1689, 3388
TSA1-F4	348i, 237, 461, 501, 526, 729, 787, 1775, 3432
TSA2-C2	323i, 220, 327, 407, 601, 666, 1116, 1676, 1973
TSA2-C4	425i, 144, 259, 291, 602, 713, 1570, 1628, 2059
TSA2-D2	178i, 266, 395, 494, 586, 738, 1319, 1512, 2049
TSA2-F3	550i, 189, 327, 446, 573, 667, 235, 1583, 2039
TSA3-B2	410i, 80, 100, 245, 455, 684, 888, 1941, 2054
TSA3-C1	124i, 75, 209, 358, 537, 831, 1105, 1805, 3238
TSA4-B2	964i, 139, 176, 215, 411, 702, 899, 1656, 1753
TSC1-C3	301i, 56, 202, 301, 551, 699, 886, 1737, 2054
TSC1-F1	304i, 228, 316, 395, 704, 774, 874, 1622, 3197
TSC2-F4	1142i, 310, 354, 572, 713, 726, 1008, 1461, 2467
TSC5-F4	132i, 310, 621, 677, 775, 994, 1246, 1594, 3235
TSD1-F4	465i, 434, 540, 768, 834, 955, 1121, 1484, 3202
TSD2-F5	831i, 305, 368, 515, 612, 646, 1181, 1470, 2073
TSF1-F2	656i, 324, 325, 485, 580, 699, 791, 1396, 2680

Isomers D1 and D2 are both of  $C_s$  symmetry with the  $^2A''$  electronic state. However, the isomer, with H bonded with the neighbor C of Si, cannot be found.

Among the six initially supposed structures, five isomers containing bridge-bonds were located. F1 (47.53 (48.06)), F2 (95.15 (98.88)), and F3 (68.68 (65.30)) possess Si–C bridge-bonds, whereas C–C bonds act as bridge-bonds in F4 (9.41 (11.20)) and F5 (49.14 (47.83)). Isomers F2 and F3, with branches bonded with the bridge-atom, stand at higher levels on PES, while F1, F4 and F5, whose H atoms bond with non-bridge-atoms, have lower energies, and moreover, the energies of the isomers with C as the bonding non-bridge atoms are relatively lower. F4 is  $C_{2v}$  symmetrized with the  $^2B_1$  electronic state, while other four planar isomers have a  $^2A''$  electronic state.

Besides, there is a point needed to note that no triangular cone (G) isomer is located despite that two geometries were designed before numerous searches.

Since the lowest lying quartet linear state was found to lie more than 39.12 kcal/mol above A1 ( $^2\Pi$ ) at the CCSD(T)/6-311G(2df, 2p)//B3LYP/6-311G(d, p) + ZPE, the quartet species and higher spin states were not considered further in the present work.

For the purpose of comparison, the geometry of linear  $C_4H$ , isovalent analogue of low-lying  $\text{SiC}_3\text{H}$  isomer A1, is also optimized at the CCSD(T)/6-311G(2df, 2p)//B3LYP/6-311G(d, p) level. However,  $C_{\infty v}$  symmetrized structure with all real frequencies was not found. Linear  $C_4H$  has an imaginary frequency, which corresponds to the C–C–C bending vibration model.

**Table 3** The energies (kcal/mol) of all the isomers at various levels

Isomers	MP2+ZPE (a.u.)	CCSD(T)+ZPE (a.u.)	G3MP2+ZPE (a.u.)	Er(CCSD(T)) (kcal/mol)	Er(G3MP2) (kcal/mol)
A1( $^2\Pi$ )	-404.2653	-403.5349	-403.6186	0	0
A2( $^2A'$ )	-404.1931	-403.4649	-403.5469	43.93	45.86
A3( $^2A''$ )	-404.1434	-403.4009	-403.4816	84.09	86.87
A4( $^2A''$ )	-404.1489	-403.4170	-403.4954	74.01	78.19
B1( $^2A''$ )	-404.1702	-403.4439	-403.5291	57.10	57.07
B2( $^2A''$ )	-404.0754	-403.3597	-403.4501	109.93	106.61
C1( $^2A''$ )	-404.1401	-403.3992	-403.4790	85.15	88.46
C2( $^2A''$ )	-404.2349	-403.5079	-403.5925	16.94	17.26
C3	-404.1156	-403.3974	-403.4793	86.31	88.28
C4	-404.1687	-403.4419	-403.5352	58.36	53.23
C5( $^2A''$ )	-404.2219	-403.4969	-403.5793	23.85	25.48
D1( $^2A''$ )	-404.2231	-403.4939	-403.5783	25.73	26.15
D2( $^2A''$ )	-404.1499	-403.4299	-403.5132	65.89	67.00
F1( $^2A''$ )	-404.1797	-403.4592	-403.5434	47.53	48.06
F2( $^2A''$ )	-404.1073	-403.3833	-403.4624	95.15	98.88
F3( $^2A'$ )	-404.1504	-403.4255	-403.5159	68.68	65.30
F4( $^2B_1$ )	-404.2496	-403.5199	-403.6022	9.41	11.20
F5( $^2A'$ )	-404.1834	-403.4566	-403.5438	49.14	47.83

The symbols in parentheses denote the electronic states

**Table 4** The energies (kcal/mol) of all the transition states at various levels

TSSs	MP2+ZPE (a.u.)	CCSD(T)+ZPE (a.u.)	G3MP2+ZPE (a.u.)	Er(CCSD(T)) (kcal/mol)	Er(G3MP2) (kcal/mol)
TSA1-C5( $^2A''$ )	-404.1899	-403.4629	-403.5492	45.18	43.56
TSA1-C5*( $^2A''$ )	-404.1725	-403.4429	-403.5298	57.73	55.73
TSA1-F4( $^2A''$ )	-404.1684	-403.4408	-403.5330	58.99	53.73
TSA2-C4	-404.1590	-403.4329	-403.5142	64.01	65.53
TSA2-D2	-404.1473	-403.4258	-403.5105	68.40	67.86
TSA2-F3	-404.1439	-403.4219	-403.5065	70.91	70.36
TSA3-B2( $^2A''$ )	-404.0788	-403.3587	-403.4457	110.56	108.52
TSA3-C1	-404.1043	-403.3872	-403.4648	92.71	96.48
TSA4-B2	-404.0764	-403.3527	-403.4495	114.33	106.14
TSC1-C3( $^2A''$ )	-404.1096	-403.3906	-403.4761	90.54	89.43
TSC1-F1( $^2A''$ )	-404.1315	-403.3938	-403.4744	88.52	90.46
TSC2-F4( $^2A''$ )	-404.1677	-403.4419	-403.5235	58.36	59.66
TSC5-F4( $^2A''$ )	-404.2204	-403.4969	-403.5786	23.85	25.10
TSD1-F4( $^2A''$ )	-404.2094	-403.4849	-403.5790	31.38	24.85
TSD2-F5	-404.1379	-403.4179	-403.5018	73.42	73.31
TSF1-F2( $^2A''$ )	-404.1005	-403.3778	-403.4588	98.56	100.29

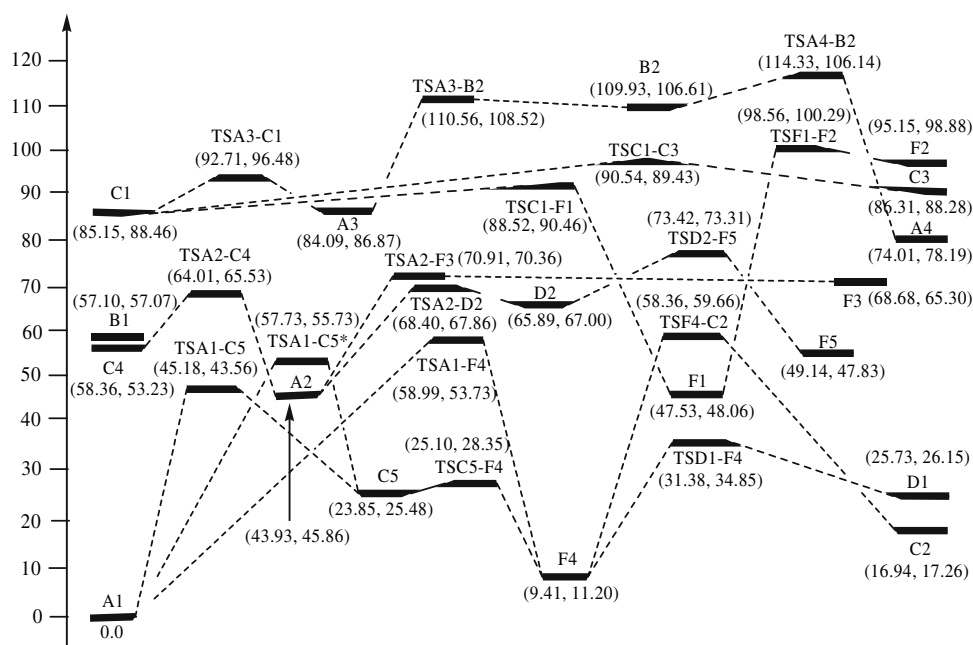
The symbols in parentheses denote the electronic states

### 3.2 SiC<sub>3</sub>H isomerization and isomer stability

The harmonic vibrational frequencies as well as the infrared intensities of relevant species at the B3LYP/6-311G(d, p) level are listed in Table 1. The number of imaginary frequency (0 or 1) confirms whether a local minimum or

a transition state. The relative energies of the dissociation products observed in the interstellar space or in the laboratory were so high that we did not put effort to investigate the transition states in the dissociation. Therefore, the kinetic stability of SiC<sub>3</sub>H isomers is primarily controlled by the isomerization barriers.

**Fig. 4** Schematic potential energy surface of SiC<sub>3</sub>H isomerizations at the CCSD(T)/6-311G(2df, 2p)//B3LYP/6-311G(d, p) level. The values in the parentheses are at the CCSD(T)/6-311G(2df, 2p)//B3LYP/6-311G(d, p) + ZPE and G3(MP2)//B3LYP/6-311G(d, p) + ZPE levels, respectively

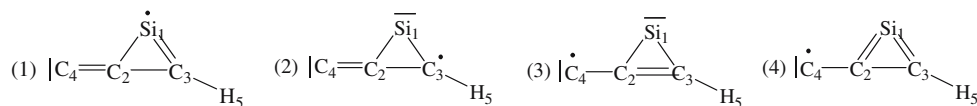


From Fig. 4, we can see that A1, A2, A4, C2, F1, F4 and F5 have relatively higher kinetic stability. At the CCSD(T)/6-311G(2df, 2p) B3LYP/6-311G(d, p) level, the linear A1 is the lowest lying isomer with considerable kinetic stability as 45.18 (43.56) kcal/mol (A1→C5). The three-membered-ring isomer, C2, also has a considerably kinetic stability of 41.42 (42.40) kcal/mol. The respective kinetic stabilities of chainlike isomers, A2 and A4, are 20.08 (19.67) (A2→C4) and 40.32 (27.95) kcal/mol (A4→B2). Besides, F1, F4 and F5 have kinetic stabilities of 40.99 (42.40) (F1→C1), 15.69 (17.15) (F4→C5) and 24.28 (25.48) (F5→D2) kcal/mol, respectively. These isomers have high enough kinetic stability to exist under low temperature conditions, such as in dense interstellar clouds. Our conclusion that linear SiC<sub>3</sub>H isomer A1 possesses a highest stability is in good agreement with those of similar systems, SiC<sub>3</sub>P [25] and SiC<sub>3</sub>N [26].

### 3.3 Property of important species

Another important and interesting issue is the bonding properties of kinetically stable isomers. For the most stable isomer, A1, the Si–C bond length is 1.698 Å. The C–H bond length, 1.063 Å, is close to that of CH<sub>4</sub>, 1.09 Å. According to atomic Mulliken spin densities (0.204, 0.524, –0.180, 0.471 and –0.018e for Si<sub>1</sub>, C<sub>2</sub>, C<sub>3</sub>, C<sub>4</sub> and H<sub>5</sub>, respectively), we can deduce that among the three possible resonant structures, (1)  $\bullet|\text{Si}-\text{C}\equiv\text{C}-\text{C}|-\text{H}$ , (2)  $|\text{Si}=\text{C}\bullet-\text{C}\equiv\text{C}-\text{H}$ , and (3)  $|\text{Si}=\text{C}=\text{C}=\text{C}\bullet-\text{H}$ , resonant structure (2) bears the most weight and (1) the least. The symbols “•” and “|” denote the unpaired single electron and lone-pair electrons, respectively.

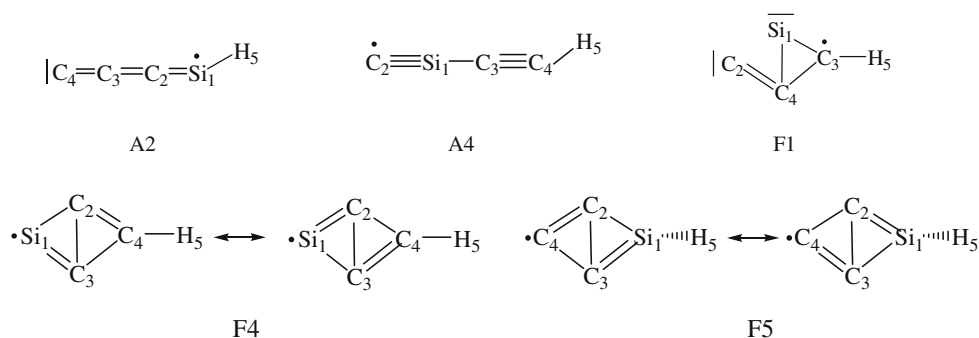
For the second stable isomer C2, the atomic Mulliken spin density distribution is 0.080, –0.030, 0.403, 0.565 and –0.017e for Si<sub>1</sub>, C<sub>2</sub>, C<sub>3</sub>, C<sub>4</sub> and H<sub>5</sub>, respectively. Considering the bond lengths (in Fig. 1), isomer C2 can be described as the following three resonant structures:



Other isomers, A3, B2, C1, C3, C4, C5, D1, D2, F3 and F2 are less kinetically stable. The isomerization barriers of these species are 8.62 (9.67) (A3→C1), 0.63 (1.91) (B2→A3), 3.37 (2.00) (C1→F1), 4.23 (1.12) (C3→C1), 5.65 (12.3) (C4→A2), 1.25 (2.87) (C5→F4), 5.65 (8.70) (D1→F4), 2.51 (0.86) (D2→A2), 2.23 (5.06) (F3→A2) and 3.41 (1.41) (F2→F1) kcal/mol, respectively.

In the view of spin density distribution and stability, (3) is considered to bear the most weight. The atomic Mulliken spin density distributions (for the corresponding atom labels, please see Fig. 1) for Si<sub>1</sub>, C<sub>2</sub>, C<sub>3</sub>, C<sub>4</sub> and H<sub>5</sub> in other isomers are 0.982, –0.239, 0.198, –0.032 and 0.091e (A2), 0.013, 0.943, –0.037, 0.084 and –0.03 (A4), –0.052, 0.538, –0.098, 0.643, –0.031 (F1), 0.688, –0.042, –0.042, 0.419

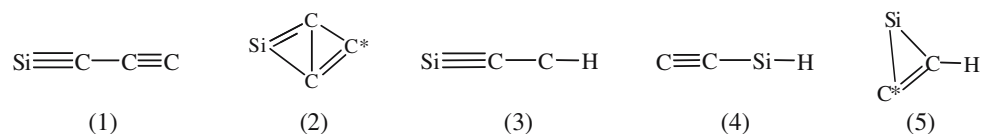
and  $-0.022$  (F4) and  $0.058$ ,  $0.021$ ,  $0.021$ ,  $0.546$  and  $-0.06$  (F5). Analogically, the resonant structures with the most weight for other kinetically stable isomers can be deduced as follows:



### 3.4 Interstellar and laboratory implications

The dipole moments and rotational constants for  $SiC_3H$  at the B3LYP/6-311G(d, p) level are listed in Table 1. As seen in Table 1, of the seven kinetically stable isomers, F5, A1, F4, A4, F1, C2 and A2, the former two have rather small dipole moments ( $0.2266$  and  $0.7731$  D, respectively) and their characterization may be identified by infrared spectrum; the latter five have rather large dipole moments as  $1.5837$ ,  $2.7981$ ,  $3.8867$ ,  $3.5508$  and  $5.1695$ , respectively, making them promising for microwave detection.

$SiC_3$  has been detected in the interstellar space [12] and in the laboratory [17] as well, with the promising forms of rhombus [12, 17] and linetype [9] (see the scheme below).  $SiC_2H$  radical possesses three potential forms, linear  $SiCCH$  and  $CCSiH$ , along with cyclic structure [8, 10] (see the scheme below).



Therefore, a large amount of dissociative H atoms in the interstellar space makes it possible to form isomer A1 by adding H atom to the terminal C of chainlike  $SiC_3$  (1). Si or  $C^*$  atom of rhomboidal  $SiC_3$  (2) binding with dissociative H may lead to the generation of F4 and F5, respectively. The addition of dissociative C to terminal Si or C of linear  $SiCCH$  (3) and  $CCSiH$  (4) can generate A4 and A2, respectively. The feasible formation mechanism of C2 and F1 is that C atom bonds with  $C^*$  atom of cyclic  $SiC_2H$  (5).

In addition,  $SiC_2H$  has been generated in the laboratory by the photolysis of a mixture of  $SiH_4$ ,  $C_2H_2$  and Ar [8]. Therefore, it is reasonable to expect that  $SiC_3H$  may be produced by similar means with SiC and  $C_2H_4$ .

## 4 Conclusions

DFT and ab initio method were employed to study the structures, energies, dipole moments, rotational constants, and

isomerization of the  $SiC_3H$  molecule. A total of 18 minima, including chain-like species (A), branched species (B), three-membered-ring species (C), four-membered-ring species (D), tetrahedron species and bridge-bond containing species (F), and 16 transition states as well on the isomerization PES were located at the CCSD(T)/6-311G(2df, 2p)//B3LYP/6-311G(d, p) level. The lowest lying isomer, linear A1, is the most kinetically stable, with the dominant resonant structures  $|Si=C-C \equiv C-H$ . The three-membered-ring isomer C2 holds the second highest kinetic stability. In addition, two chain-like isomers (A2 and A4) and three bridge-bond containing isomers (F1, F4 and F5) also have considerably high kinetic stability. Other high-energy isomers, A3, B2, C1, C3, C4, C5, D1, D2, F3 and F2 are also less kinetically stable. Of those, F4, A4, F1, C2 and A2 are promising for microwave detection with larger dipole moments. Due to the small dipole moments, F5 and A1 can be identified by infrared spectrum.

**Acknowledgments** This work is supported by the National Natural Science Foundation of China (No.20773021) and the Science Foundation for Young Teachers of Northeast Normal University (No. 20070-315). We are greatly thankful for the referees' helpful comments.

## References

- Furthmuller J, Bechstedt F, Husken H et al (1998) Si-rich  $SiCC(111)/(0001)3 \times 3$  and  $3 \times 3$  surfaces: a Mott-Hubbard picture. *Phys Rev B* 58:13712–13716
- Frost S, Murphy WJ, Roberts MW et al (1972) Mechanism of formation and some surface characteristics of thin polymer films



- formed on metal surfaces by electron bombardment. *Faraday Special Discuss Chem Soc* 2:198–209
- Carlsson A Jr, Clevenger L, Madsen LD et al (1997) Phase formation sequences in the silicon–phosphorus system: determined by in-situ synchrotron and conventional X-ray diffraction measurements and predicted by a theoretical model. *Philos Mag B* 75:363–376
  - Ding YH, Li ZS, Huang XR et al (2001) Theoretical study on potential energy surface of the interstellar molecule SiC<sub>2</sub>N. *J Phys Chem A* 105:5896–5901
  - Cheng X, Xie Z, Song Y et al (2006) Structure and properties of polycarbosilane synthesized from polydimethylsilane under high pressure. *J Appl Polym Sci* 99:1188–1194
  - Taki T (1992) Solid-state nuclear magnetic resonance (NMR): application to precursors of ceramics—polycarbosilane. *J Inorg Organomet Polym* 2:269–279
  - McCarthy MC, Apponi AJ, Gottlieb CA (2001) Rotational spectra of SiCN, SiNC, and the SiC<sub>n</sub>H(*n* = 2, 4–6) radicals. *J Chem Phys* 115:870–877
  - Han DS, Rittby CML, Graham WRM (1997) Fourier transform infrared observation of the vibrational spectrum of the linear SiCCH radical in Ar at 10 K. *J Chem Phys* 106:6222–6230
  - Jiang ZY, Xu XH, Wu HS et al (2002) Structure and stability of Si<sub>n</sub>C<sub>m–n</sub> clusters. *J Mol Struct (Theochem)* 589–590:103–109
  - Largocaberizo A, Flores JR (1988) A preliminary theoretical study of the SiC<sub>2</sub>H radical: implications in astrophysics. *Chem Phys Lett* 147:90–94
  - Redondo P, Saguillo A, Barrientos C et al (1999) Theoretical study of the reaction of Si<sup>+</sup> with C<sub>3</sub>H<sub>2</sub>. *J Phys Chem A* 103:3310–3320
  - MacKay DDS, Charnley SB (1999) The silicon chemistry of IRC+10 degrees 216. *Mon Not R Astron Soc* 302:793–800
  - Herbst E, Millar TJ, Wlodek S, Bohme DK (1989) The chemistry of silicon in dense interstellar clouds. *Astron Astrophys* 222:205–210
  - McCarthy MC, Gottlieb CA, Thaddeus P (2003) Silicon molecules in space and in the laboratory. *Mol Phys* 101:697–704
  - Guelin M, Muller S, Cernicharo J et al (2000) Astronomical detection of the free radical SiCN. *Astron Astrophys* 363:L9–L12
  - Apponi AJ, McCarthy MC, Gottlieb CA et al (1999) The rotational spectrum of rhomboidal SiC<sub>3</sub>. *J Chem Phys* 111:3911–3918
  - Winnewisser G (1997) Interstellar and laboratory spectroscopy in the terahertz region. *J Mol Struct* 408:1–10
  - McCarthy MC, Apponi AJ, Thaddeus P (1999) Rhomboidal SiC<sub>3</sub>. *J Chem Phys* 110:10645–10648
  - Bell MB, Feldman PA, Watson JKG et al (1999) Observations of long C<sub>n</sub>H molecules in the dust cloud TMC-1. *Astrophys J* 518:740–747
  - Apponi AJ, McCarthy MC, Gottlieb CA et al (2000) The radio spectra of SiCCH, SiCN, and SiNC. *Astrophys J* 536:L55–L58
  - Frisch MJ, Trucks GW, Schlegel HB et al (2003) Gaussian, Pittsburgh
  - Becke AD (1993) Density-functional thermochemistry. III. The role of exact exchange. *J Chem Phys* 98:5648–5652
  - Lee C, Yang WT, Parr RG (1988) Development of the Colle-Salvetti correlation-energy formula into a functional of the electron density. *Phys Rev B* 37:785–789
  - Becke AD (1992) Density-functional thermochemistry. I. The effect of the exchange-only gradient correction. *J Chem Phys* 96:2155–2160
  - Liu HL, Huang XR, Chen GH, Ding YH, Sun CC (2004) Theoretical Study on the Structures and Stability of SiC<sub>3</sub>P Isomers. *J Phys Chem A* 108:11828–11837
  - Liu HL, Huang XR, Chen GH, Ding YH, Sun CC (2004) SiC<sub>3</sub>N: A promising interstellar molecule with stable cyclic isomers. *J Phys Chem A* 108:6919–6927
  - Liu HL, Ding YH, Huang XR, Sun CC (2006) Theoretical study on PCCCP and its isomers. *J Mol Struct: THEOCHEM* 759:209–213
  - McLean AD, Chandler GS (1980) Contracted Gaussian basis sets for molecular calculations. I. Second row atoms, Z=11–18. *J Chem Phys* 72:5639–5648
  - Krishnan R, Binkley JS, Seeger R, Pople JA (1980) Self-consistent molecular orbital methods. XX. A basis set for correlated wave functions. *J Chem Phys* 72:650–654
  - Fukui K, Kato S, Fujimoto H (1975) Constituent analysis of the potential gradient along a reaction coordinate. Method and an application to methane + tritium reaction. *J Am Chem Soc* 97:1–7
  - Gonzalez C, Schlegel HB (1989) An improved algorithm for reaction path following. *J Chem Phys* 90:2154–2161
  - Gonzalez C, Schlegel HB (1990) Reaction path following in mass-weighted internal coordinates. *J Phys Chem* 94:5523–5527
  - Ignatyev IS, Xie YM, Allen WD, Schaefer HF (1997) Mechanism of the C<sub>2</sub>H<sub>5</sub> + O<sub>2</sub> reaction. *J Chem Phys* 107:141–155
  - Schlegel HB, Sosa C (1988) Ab initio molecular orbital calculations on F + H<sub>2</sub> → HF + H and OH + H<sub>2</sub> → H<sub>2</sub>O + H using unrestricted Møller-Plesset perturbation theory with spin projection. *Chem Phys Lett* 145:329–333